Acoustic emission characteristics and mechanical responses of rock specimens during direct tensile test

Ruifu YUAN[2], Zhiqiang HOU[2]

Abstract. To understand the laws of mechanical response and acoustic emission (AE) activities in the tension process of rock specimens, the directly tensile test, tensile cyclic loading test and uniaxial compressive test were conducted on three kinds of rock specimens and the AE signals were monitored. The fast Fourier transformation (FFT) method was used to analyze the frequency spectrum characteristics of AE signals. Compared with the compressive loading test on rock specimens, no obvious yield stage was found in the directly tensile stress-strain curve and the AE events were relatively less in quantity and small in energy. The macro failure occurred very suddenly and the high-energy AE events only occurred around the failure moment of rock specimens without obvious precursory information. The tensile tangent modulus gradually decreased with the increasing of stress and the occurrence of AE activities corresponded to the decreasing of tangent modulus. The stress-strain curve became non-linear when reloading level exceeded the previous loading level. Meanwhile, the clear Kaiser effect of AE activity could be observed in each cyclic loading. Whichever frequency bands the peak frequency was at, the spectrum had absolute advantages and was easy to distinguish for its relatively simple distribution of AE in the tensile test. It indicated that the focal mechanism of AE signals was relatively simple under the direct tensile state and the signals were mainly produced by the tensile failure of single couple source parallel to the axial direction of the specimen.

Key words. Rock specimen; direct tensile test; acoustic emission; cyclic loading; tangent modulus.

1. Introduction

Measuring acoustic emissions (AE) or microseismic has already become an important technique for studying the damage caused to rocks as well as for evaluating the

[2] Workshop 1 - School of Energy Science and Engineering, Henan Polytechnic University, Jiaozuo City, Henan Province 454003; e-mail: yrf@hpu.edu.cn

stability of rock mass engineering structures because it allows for the real-time monitoring of the signals generated when rocks are damaged by an external force or agent [1-5]. Rocks, which are naturally formed geologic materials, contain mineral grains, pores, and fissures in complex distributions and exhibit strongly heterogeneous characteristics. During the loading of rock specimens, AE are generated because of the damage incurred by the inner particles, as well as owing to slippage, friction, the closing or expansion of existing fissures, and the formation of new ones. Meanwhile, thousands of AE events occur even during tests performed on small rock specimens in the laboratory. The AE signal is influenced by a number of factors, including the characteristics of the rock specimen in question, its stress state, the monitoring equipment used, and the external environment. Therefore, the AE signal contains complex information, and it remains a challenge to identify the characteristics of the AE signal and use this information to determine the damage incurred by the inner parts of the rock specimen.

The above-mentioned studies indicate that the AE of rocks under direct tension are markedly different from those of rocks under compressive stress. Further, the AE occur primarily before the total failure of the test specimen and are short-lived, suggesting that it would be more difficult to capture preliminary AE data in the case of tensile-damaged rocks. Although engineering rock mass is mostly under compressive stress, in many cases, the damage incurred by rock mass engineering structures is initiated in the parts under tensile stress, owing to the low tensile strength of rocks. If the monitored AE signal could be used for evaluating the tensile damage incurred by rocks, it would allow one to determine the stability of rock mass engineering structures with greater accuracy. Therefore, in this study, we attempted to monitor the AE characteristics of different types of rocks subjected to the direct tensile and cyclic tensile tests. Moreover, the uniaxial compressive test was also conducted, in order to analyse the differences in the characteristics of the AE signals as well as the AE activities of rock specimens subjected to tensile and compressive stresses.

2. Test setup and methods

Two problems must be overcome when performing the direct tensile test on rock specimens. To begin with, the cohesive force between the pull head and the test specimen must be high enough to break the specimen. Next, the pull rod, pull head, and specimen axes should be centered, so that the direction of the tensile stress is completely parallel to the central axis of the specimen and there is no eccentricity. Therefore, a pair of spherical hinge pull heads was used to eliminate all unevenness on both ends of the test specimen and ensure that the tensile stress was applied at the center. A threaded force-delivering steel cap was used to connect the test specimen and the spherical hinges: one end of the threaded cap was connected to the pull head, while the other end was stuck to the specimen; this end had a smooth surface and was same in size to the specimen's end. An acrylate adhesive with a tensile strength of 24 MPa was used to stick the steel cup and the test specimen together.

The test specimens used were drilled from the base material, which were white coarse-grained marble, black fine-grained marble and coarse sandstone. The drilled samples were processed into standard-sized samples with dimensions of 50 mm (diameter) $\times$ 100 mm (length), in accordance with the ISRM standard[9].The sensors should correspond to each other between the top end and the bottom end of the specimen, as shown in Figure. 1.
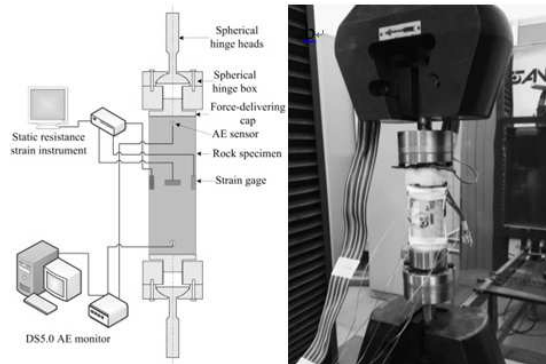

Fig. 1. Diagram and photograph of the setup used for the direct tensile test. a – Schematic diagram of test setup, b – Photograph of test specimen in setup

3. Test results

3.1. Mechanical properties of rock specimens

The mechanical properties of the three types of rock specimens used in this study (white coarse-grained marble, black fine-grained marble and coarse sandstone) were determined; the results are shown in Table 1.

Table 1 Mechanical properties of the three types of rocks tested

Test condition	Lithological character	Serial number	Density ρ/kg m^{-3}	Longitudinal wave velocity v_p/(m.s^{-1})	Compressive elastic modulus E_c/(GPa)	Uniaxial compressive strength (UCS) σ_c/MPa	Uniaxial tensile strength (UTS) σ_t/MPa
Compression test	Fine-grained marble	Average value of A Group	2703	4863	37.0	85.0	——
	Coarse-grained marble	Average value of B Group	2732	5526	71.3	130.4	——
	Coarse sandstone	Average value of C Group	2427	3000	24.1	85.7	
Tension test	Fine-grained marble	A1	2715	4667	——	——	4.2
		A2	2718	4651	——	——	3.7
		A3	2707	4794	——	——	3.2
		A4	2705	4811	——	——	4.1
		A5	2718	4609	——	——	2.5
		Average value	2713	4706			3.5
	Coarse-grained marble	B1	2726	5587	——	——	7.2
		B2	2689	5692	——	——	7.5
		B3	2708	5622	——	——	7.3
		B4	2713	5275	——	——	4.6
		B5	2732	5087	——	——	5.8
		Average value	2714	5453			6.5
	Coarse sandstone	C1	2424	2616	——	——	1.9

It can be seen that all three types of rocks tested were moderately hard rocks, with the coarse-grained marble exhibiting the highest strength and elastic modulus. Further, the average uniaxial compressive strength (UCS) of these specimens was 130.4 MPa, and their average uniaxial tensile strength (UTS) was 6.5 MPa, with the UCS/UTS ratio being 14.8. For the fine-grained marble specimens, the average UCS and UTS values were 85.0 MPa and 3.5 MPa respectively, with the UCS/UTS ratio being 25.4. Finally, for the coarse sandstone specimens, the average UCS and UTS values were 85.7 MPa and 4.1 MPa respectively, with the UCS/UTS ratio

Fig. 2. Photographs of failed specimens after the direct tensile and uniaxial
compressive tests. a – After direct tensile test, b – After uniaxial compressive test

being 24.9. It can be seen from the photographs of the failed specimens (see Fig. 2)
that most of the specimens subjected to the uniaxial compressive test exhibited shear
failure, which was accompanied by the partial splitting of the specimens. In contrast,
the damage experienced by the specimens subjected to the direct tensile test was
relatively simpler. The failure positions and morphologies of these samples were
irregular. The fine-grained marble samples failed near one of their ends. Further,
the failure surface was even and almost perpendicular to the tensile direction.

3.2. AE activities under uniaxial compression

Figure 3 shows the distributions of the AE activities for the three types of rocks
under uniaxial compression. A large number of AE events were observed during the
loading process for all three types of specimens. AE signals were observed primarily
during two stages: the compaction stage and the yielding stage of the specimens.
The AE activities of all the specimens remained stable during elastic deformation
stage. Further, even though a large number of AE events were observed during the
compaction stage, most of the AE events were low energy. On the other hand, the
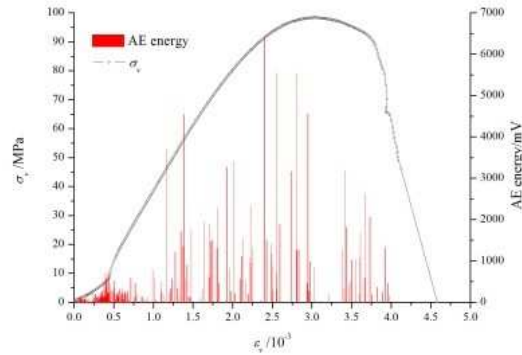AE events in the yielding stage produced high-energy AE.

Fig. 3. AE activities of the three types of rock specimens under uniaxial compression. a – Fine-grained marble, b – Coarse-grained marble, c – Coarse sandstone

3.3. AE activities under direct tension

Figure 4 shows the distributions of the AE activities of the three types of specimens as observed during the direct tensile test. For all the rock types, no obvious yield stage was observed in the stress–strain curve obtained from the direct tensile test. Moreover, all the specimens failed suddenly, and the test equipment was unable to monitor the post-peak curve. Fewer AE events were observed during the direct tensile test than was the case during the compressive test. Further, it was difficult to monitor the AE events in the initial tensile loading stage. For the two types of marble specimens, only low-energy AE signals were recorded, with the signals lasting only for the active stage before failure until the loading stress reached 30% of the tensile strength. For the sandstone specimens, only a few sporadic AE events were recorded during the entire loading process, with AE activity being observed only at the moments the specimens failed.

The tensile stress–strain curves for all three rock types were shallow convex, suggesting that the tangent modulus of elasticity, E_t, decreased gradually with an increase in the applied tensile stress. For the coarse-grained marble specimens, a distinctly linear portion was observed in the stress–strain curve in the initial loading stage; however, the curve became nonlinear once the tensile stress exceeded 30% of the tensile strength. At this moment, AE events started occurring, indicating the generation of tensile cracks within the specimens and a gradual decrease in the number of microscale grains that could bear the tensile stress. For the fine-grained marble specimens, the entire stress–strain curve was nonlinear, and the AE events occurred in the initial loading stage, indicating that the inner grains of these specimens were inhomogeneous in terms of their tensile strength. As was the case for the coarse-grain marble specimens, the occurrence of the AE signals corresponded to changes in the curvature of the stress–strain curve. Finally, the coarse sandstone used had a more complex internal structure, consisting of cements, grains, and cracks. Thus, the tensile stress–stain curve for these specimens consisted

of two distinct stages, as can be seen from Figure. 4(c). In the first stage, the stress–strain curve exhibited a large curvature, and only low-energy AE events were observed; these were related to the generation of cracks in the cements between the grains (see Figure. 5).
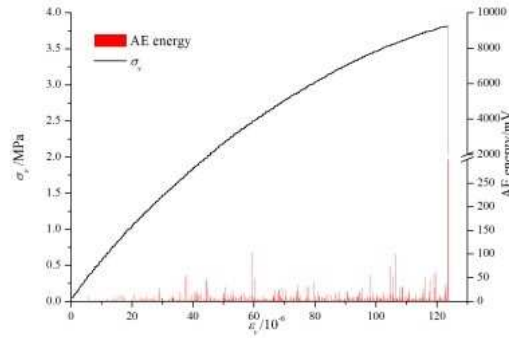

Fig. 4. AE activities and stress–stain curves for various rock specimens during direct tensile test. a – Fine-grained marble, b – Coarse-grained marble, c – Coarse sandstone
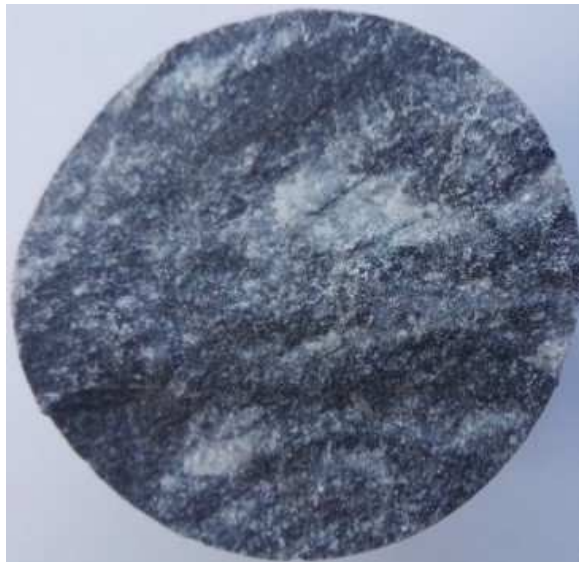

Fig. 5. Tensile-fractured surfaces of specimens of the three types of rocks tested. a – Fine-grained marble, b – Coarse-grained marble, c – Coarse sandstone

3.4. Results of cyclic direct tensile loading tests

Figure 6 shows the stress–strain curves obtained from the cyclic direct tensile loading tests performed on the three types of rocks. Cyclic tensile loading had little effect on the tensile strengths of the rock specimens or on the curvatures of their stress–strain curves. It can be seen that the tensile loading and unloading processes were non-repeatable and similar to cyclic uniaxial compressive loading. During the reloading process, the stress–strain curve was linear when the loading level was lower than that for the previous loading cycle but became nonlinear when the loading stress exceeded that for the previous loading cycle, indicating that the tangent modulus decreased with an increase in the tensile stress. During the unloading process, on the other hand, the stress–strain curves were nearly linear for every loading cycle; this was true for all three types of specimens. Although the three types of specimens
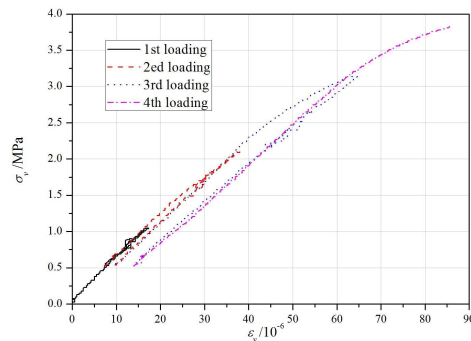

Fig. 6. Stress–strain curves for three types of specimens under cyclic tensile
loading. a – Fine-grained marble, b – Coarse-grained marble, c – Coarse sandstone

showed significant differences in their material properties, their mechanical responses under cyclic tensile loading were similar. Their inner cracks increased in number and size under tensile loading, with the generation of the cracks resulting in a decrease in the number of grains which could still bear the tensile stress. As a result, the tangent modulus decreased gradually, as can be seen from the stress–strain curves. During the unloading process, only the undamaged grains remained resilient, with the damaged ones being unable to recover which consume parts of energy in the loading process. During the reloading process, the number of grains that could bear the tensile stress was lower than that during the previous loading process. Hence, the tensile elastic modulus decreased with an increase in the number of loading cycles. Figure 7 shows the tensile elastic moduli of the three types of rock specimens under different cyclic loads. It can be seen that the decrease in the elastic moduli of the marbles, which were homogeneous and solid, was smaller than that in the case of the coarse sandstone, which was nonhomogeneous and porous. This indicated that the previous loading cycles caused less damage in the marble specimens than in the sandstone specimens. Figure 8 shows the relationship between the stress and
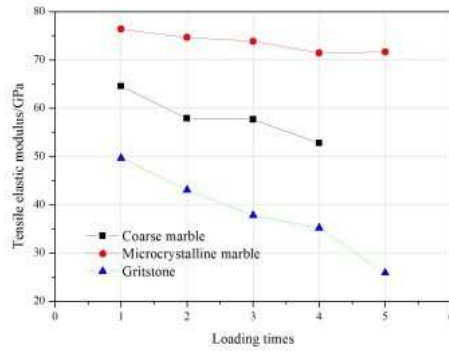
Fig. 7. Variations in tensile elastic moduli of three types of specimens during
cyclic tensile loading

energy accumulation corresponding to the AE events during cyclic tensile loading.
The points labeled KE in Figure. 8 refer to the points at which the Kaiser effect
was observed; that is to say, the points at which AE activities were observed again
during repeated loading. It can be seen that the Kaiser effect was pronounced for
all three types of rock specimens. The AE signals reappeared only when the loading
stress exceeded the maximum stress during the previous loading cycle. On the other
hand, no AE signals were observed during the unloading process. The fact that the
Kaiser effect was observed during cyclic loading confirmed that the inner structures
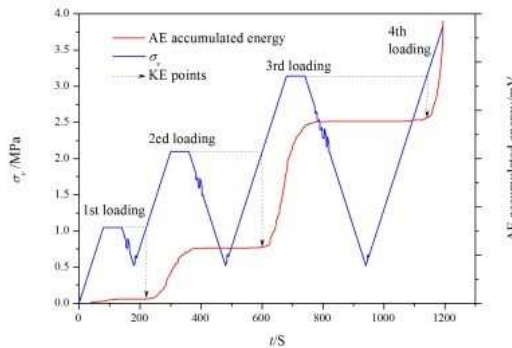of the rock specimens were progressively damaged during the tensile test.

Fig. 8. Relationships between stress and accumulation of AE energy during cyclic
tensile loading. a – Fine-grained marble, b – Coarse-grained marble, c – Coarse
sandstone

3.5. Waveforms and frequency spectra of AE events under compressive and tensile stresses

Figures 9 and 10 show the waveforms and frequency spectra that calculated by fast Fourier transformation (FFT) method for typical AE signals of the rock specimens under uniaxial compressive and tensile stresses. As can be seen from Figure. 9, the AE amplitude was larger during the compressive test, because the loading level during the compressive test was significantly greater than that during the tensile test. It can also be seen that a significant amount of noise (amplitude of approximately 30 mV) was present in the waveforms during the entire test. Even though this interfering noise can be filtered by processing the data after collection, the accuracy of the time of occurrence of the AE events would be affected negatively. The transmission time for the AE waves, that is, the time from their generation to the point where they reached the AE sensors, was less than 0.03 ms. This was because of the small size of the rock specimens (the maximum apparent size was approximately 112 mm (length) and the high transmission speed of the AE waves (4000–50000 m/s). Therefore, even a small error in determining the time of occurrence of AE events may cause a large deviation in the location of the AE source. The interference noise is less for the loading method and low power of the press machine in the tensile test, and the waveforms are almost straight before the arrival of AE events, making it easier to judge the arrival time of AE. Thus, the occurrence times of the AE events for the specimens under tensile stress could be determined with greater accuracy.
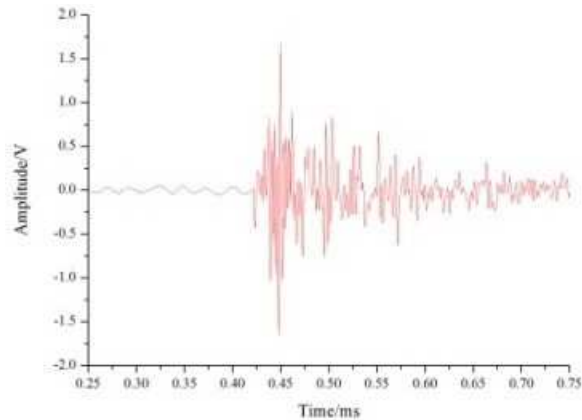

Fig. 9. Waveforms and spectra of AE signals during uniaxial compressive test. a – Waveform for AE events with low frequencies, b – Spectrum for AE events with low frequencies, c – Waveform for AE events with moderately high frequencies, d – Spectrum for AE events with moderately high frequencies

4. Discussion

The mechanical response of rocks during compressive fracturing differs greatly from that during tensile fracturing. Therefore, different theoretical models have
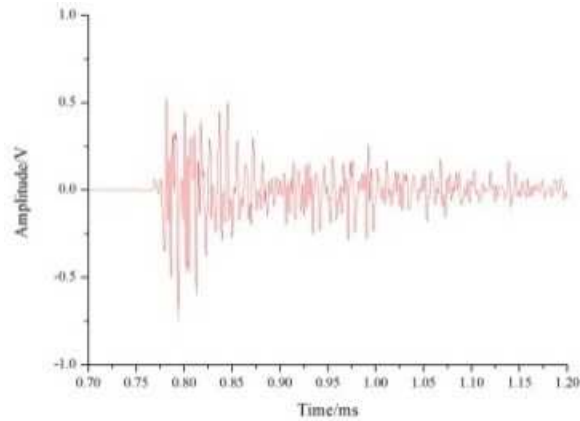
Fig. 10. Waveforms and spectra of AE signals during direct tensile test. a –
Waveform for AE events with moderately high frequencies, b – Spectrum of AE
events with moderately high frequencies, c – Waveform of AE events with high
frequencies, d – Spectrum of AE events with high frequencies

been proposed to describe their material constitutive relationship, damage evolution
mechanism, and strength criteria. A number of experimental studies also suggest
that sudden fractures are more likely to occur when rocks are under tensile stress;
this makes it difficult to capture precursory data related to the AE activities during
the tensile test. Owing to the differences in the direct tensile and compressive tests as
well as the resulting stress distributions, the fracture mechanism in the compressive
state is a complex one as compared to that in the tensile state, with the AE signals in
the latter case corresponding to the microscale tensile fractures within the rocks. The
propagation of these inner fractures is reflected in the fact that the tangent modulus
of elasticity decreases monotonically with an increase in the tensile stress, that the
tensile elastic modulus decreases during cyclic reloading, and that the Kaiser effect
is observed in these rock specimens. Therefore, one can develop tensile constitutive
models or strength criteria for rocks by treating the AE signals as being indicative
of the damage incurred.

5. Conclusions

The AE signals from three types of rock specimens during uniaxial compres-
sive and tensile tests were monitored and the characteristics of the AE signals and
the mechanical responses of the rock specimens during the tests were determined.
Further, the waveforms and spectra of the AE signals related to the compressive
and tensile states were also analyzed. The conclusions drawn in this study can be
summarized as follows:

(1)A distinct yielding stage was not observed in the stress–strain curves from
the tensile test. Further, the specimens fractured suddenly on the macroscopic
scale, with little precursory information being available. The fracture patterns of

the specimens subjected to the direct tensile test were relatively simple, with the fracture surface essentially being perpendicular to their axial direction. The stress–strain curves for all three types of rocks were shallow convex, suggesting that the tangent moduli of these specimens decreased gradually with an increase in the direct tensile stress.

(2)The number and energy of AE events observed in the case of the specimens subjected to the direct tensile test were smaller than that for the specimens subjected to the compressive test. In particular, no AE event was observed in the initial loading stage, and the AE signals were observed primarily just before the specimen fractured completely. The occurrence of the AE events corresponded to a decrease in the tangent modulus of the rock specimens.

(3)During cyclic tensile loading, the stress–strain curve was linear when the reloading level was lower than that during the previous loading cycle. Further, the elastic modulus was lower than that during the previous loading cycle. However, the stress–strain curve became nonlinear when the loading level exceeded that during the previous loading cycle; this was manifested as a decrease in the tangent modulus. On the other hand, the stress–strain curve was nearly linear during every unloading process. In addition, a distinct Kaiser effect was observed during every loading cycle.

References

[1] LIN. J,CHEN. W,SUN. L. L: *Simulation of elastic wave propagation in layered materials by the method of fundamental solutions.* Engineering Analysis with Boundary Elements *57* (2015),88–95.

[2] ZHANG. J,ZHANG. H. J,CHEN. E. H: *Real-time earthquake monitoring using a search engine method.*Nature Communications 5 (2014),1–9.

[3] DONG. L. J, LI. XIBING: *A microseismic/acoustic emission source location method using arrival times of ps waves for unknown velocity system.*International Journal of Distributed Sensor Networks (2013),1–8.

[4] MIYACHI. T: *Acoustic model of micro-pressure wave emission from a high-speed train tunnel.* Journal of Sound and Vibration*391* (2017),127–152.

[5] LIU. F,YAO. S,ZHANG. J: *Effect of increased linings on micro-pressure waves in a high-speed railway tunnel.* Tunnelling and Underground Space Technology *52*(2016),62–70.

[6] Y. F. ZHOU, Z. M. WANG: *Vibrations of axially moving viscoelastic plate with parabolically varying thickness.* J Sound and Vibration *316* (2008), Nos. 1–5, 198–210.

[7] R. LAL: *Transverse vibrations of orthotropic non-uniform rectangular plate with continuously varying density.* Indian Journal of Pure and Applied Mathematics *34* (2003), No. 4, 587–606.

[8] R. LAL, Y. KUMAR: *Transverse vibrations of non-homogeneous rectangular plates with variable thickness.* Mechanics of Advanced Materials and Structure *20*, (2013), No. 4, 264–275.

[9] Y. KUMAR: *Free vibration analysis of isotropic rectangular plates on Winkler foundation using differential transform method.* IJ Applied Mechanics and Engineering *18* (2013), No. 2, 589–597.